

Theoretical Study of the Effective Parameters for Direct Contact Membrane Distillation in Hollow Fiber Modules

Dr. Salah S. Ibrahim.

Chemical Engineering Department, University of Technology/ Baghdad.

Email: salah_salman73@yahoo.com.

Received on: 20/2/2014

&

Accepted on: 30/9/2014

ABSTRACT

The main object of this research is to study the parameters that have important effects upon performance of the direct contact membrane distillation (DCMD) process, through predicting the effects of the outside and inside diameters, the thickness of the hollow fiber membrane, the pore size, porosity, tortuosity, module length, number of fibers in module, inlet feed temperature, inlet feed concentration, inlet permeate temperature and the velocity of feed and permeate. The effective parameters that influence the performance of DCMD are classified into membrane characteristics, operating conditions, and parameters of module specifications. This study is based on an experimental system of Wang et al., 2008^[1] as typical system. It was found that the increase of the permeate flux is by selecting an optimum thickness for each inside or outside diameter of hollow fibers and an optimum number of fibers in the module and increasing the porosity and pore size within practical range and decreasing of tortuosity and as well as increasing the inlet feed temperature rather than decreasing the inlet permeate temperature for constant temperature difference between feed and permeate. Also it is found that the feed concentration and fiber length play an inverse role with the permeate flux.

Keywords: Membrane distillation; DCMD; Modeling; Desalination

دراسة نظرية للمعاملات المؤثرة على التقطير بالاغشية نوع الاتصال المباشر في وحدات الالياف المجوفة

الخلاصة

الهدف من البحث هو دراسة المعاملات التي لها تأثير مهم على اداء عملية التقطير بالاغشية نوع الاتصال المباشر من خلال التكهن بالتأثيرات للقطر الخارجي و الداخلي و سمك الجدار للليف المجوف و قطر المسامات و المسامية و التعرجية و طول الوحدة و عدد الالياف المجوفة بالوحدة بالإضافة الى السرعة و درجة الحرارة و التركيز الداخل للقيم و السرعة و درجة حرارة للمتخلل. هذه المعاملات المؤثرة على الاداء ممكن تبويبها الى مزايا و خواص الغشاء , الظروف التشغيلية و المعاملات الخاصة بمواصفات الوحدة. هذه الدراسة تمت بالاعتماد على النظام العملي و التجريبي لـ Wang et al., 2008^[1] كنظام نمونجي فيما يخص الجانب العملي. ما تم ايجاده الزيادة في التدفق عبر الاغشية يكون من خلال اختيار السمك الامثل حسب القطر الداخلي او الخارجي للغشاء المجوف و العدد الامثل للالياف المجوفة المستخدمة بالخلية مع زيادة المسامية و قطر المسامات و تقليل التعرج بالمسار عبر الغشاء و بالإضافة الى زيادة درجة الحرارة للقيم الداخل اولى من تقليل درجة حرارة سائل

التبريد عند اعتماد فارق ثابت بينهما. كذلك تم ايجاد ان التركيز للقيم وطول الالياف المستخدمة تلعب دور عكسي مع التدفق.

INTRODUCTION

Gradually, with increasing supply and demand for fresh water around the world in the last decades, saline-water desalination technology has been developing quickly. In this context, Membrane Distillation (MD) is a promising technology for desalting highly saline waters. MD is a non-isothermal separation process applied for solutions concentrated, such as desalination of seawater and brackish water.

It is still being developed at desalination testing stages and yet it is not fully implemented in industries. This process is still under evaluation, and different contradicted opinions exist concerning its features [2]. Increasing attempts are being made for scaling-up MD systems, and pilot plants have proved employed alternative energy sources, such as solar energy [3,4]. MD exhibits various advantages over the industrial well-established reverse osmoses RO process in the field of desalination. MD can treat aqueous solutions of salts with higher concentrations than sea water.

Khayet and Matsuura [10] showed that most of DCMD studies were performed to investigate the effects of the operating conditions and very few research groups have investigated the effects of membrane parameters on DCMD performance.

In the DCMD process, the feed is in a direct-contact with a surface of hydrophobic porous membrane at feed side. A thin air layer entrapped within the membrane pores comprises the gas membrane. The more volatile components evaporate from the feed at the feed/membrane interface. These vapors subsequently diffuse through the air filling the membrane pores and condense in the cold stream at permeate side (see Figure 1). A vapor pressure difference is the driving force for the mass transport which results from the temperature and composition of solutions in the layers adjoining the membrane (see Figure2)[3, 6,13-14].

Lawson and Lloyd [14] reported a familiar relationship between the membrane permeation flux (J), and different membrane characteristic in MD process may be described as follows;

$$J \propto \frac{r^\alpha \epsilon}{\delta \tau} \dots(1)$$

where r is the mean pore radius of the membrane pores, α represents the factor value, which equals to 1 or 2 for Knudsen diffusion and viscous fluxes, ϵ is the membrane porosity, δ is the membrane thickness, and τ is the membrane tortuosity.

The membrane thickness is a significant characteristic in the MD system.

According to equation (1), it is clear that there is an inversely proportional relationship between the membrane thickness and the permeate flux. The permeate flux is reduced as the membrane becomes thicker, because the mass transfer resistance increases, while the heat loss is also reduced as the membrane thickness increases. However, this inverse proportionality decays for thin membrane. This phenomenon is because of the increased conductive heat loss associated with thinner membranes [14]. Membrane porosity is an important parameter affecting MD flux. Higher porosity membranes have a larger evaporation surface area. Porosity of the

membrane is depending on the membrane polymer types and the additives. Tortuosity (τ) is simply, represented as the deviation of the pore structure from the cylindrical shape. As a result, the higher the tortuosity value, the lower the permeate flux. In fact, no systematic study had been performed on the effect of tortuosity on MD permeation flux. The values of this parameter must be evaluated experimentally, however due to the difficulties in measuring its real value experimentally for any micro-porous membrane used in MD process; the investigators frequently assume it [11].

There is a critical penetration pressure, depending on the membrane material, pore size and surface morphology, above which the liquid stream on the feed or permeate side will penetrate into the membrane. This pressure is known as the liquid entry pressure (LEP) [19]. Generally, an optimum value of the pore size is needed to be determined for each MD application depending on the type of the feed solution to be treated, and operating conditions [2, 11].

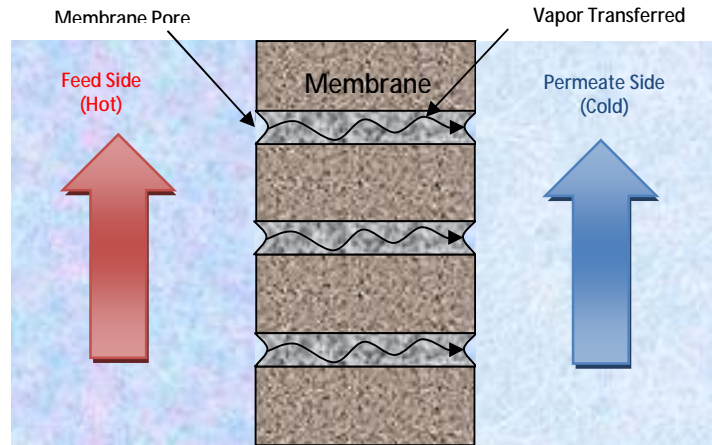
The effect of the feed temperature on the permeate flux has been widely investigated in the different cited MD configurations. The feed inlet temperature usually has been varied from 20 to 80°C in most studies [11]. In other few studies, it may be up to 85°C [12, 30] and even up to 90°C [19], in general, below the boiling point of the feed solution, maintaining all other MD parameters constant. It is well known that MD can treat highly concentrated solutions without suffering the large drop in permeability observed in other membrane processes, such as the pressure-driven membrane processes [11].

The permeate flux product is falling significantly when feed concentration increases due to decreasing vapor pressure which leads to reduced performance of MD and increasing temperature polarization [18, 30]. Working at a high feed flow rate minimizes the boundary layer resistance and enhances the heat transfer due to the maximization of the heat transfer coefficient. As a result, a higher flux and temperature polarization can be achieved [35]. There is an important effect of the flow rate of the permeate stream on the permeate flux [37]. However, Banat and Simandl [9] found a negligible influence on the permeate flux when the cold side flow rate was enhanced.

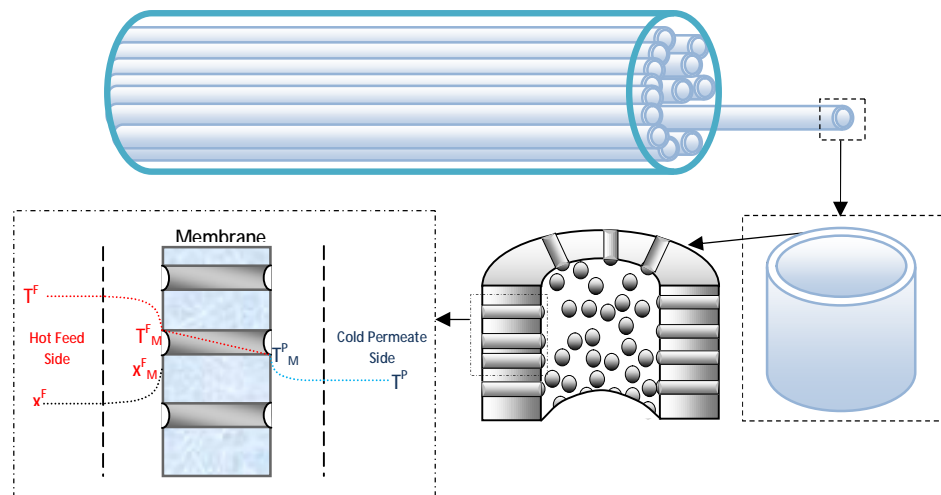
Membrane distillation is an attractive process that still requires more extensive studies for preparing it to be fully implemented in industries. These extensive studies require more focus to demonstrate clearly the effect of some parameters that may play an important role to enhance the performance of the DCMD process.

To carry out that, an extensive experimental work is required to study these parameters experimentally. In one side such as these studies require great efforts to actualize them and in another side, some effective parameters on DCMD process are not easy to study experimentally, such as tortuosity due to the difficulties in measuring its real value experimentally for any micro-porous membrane used in MD process [11]. In this matter, it is possible to bear an alternative track if this track is competent. The aim of this study is to investigate theoretically the effect of some important parameters by changing individual parameters (design parameters), on permeate fluxes.

The studied parameters include the outside and inside diameters, the thickness of the hollow fiber membrane, the pore size, porosity, tortuosity, module length, number of fibers in module, inlet feed temperature, inlet feed concentration, inlet permeate temperature and the velocity of feed and permeate streams.



Figure(1): Direct contact membrane distillation.



Figure(2):the mechanisms of heat and mass transfer in DCMD

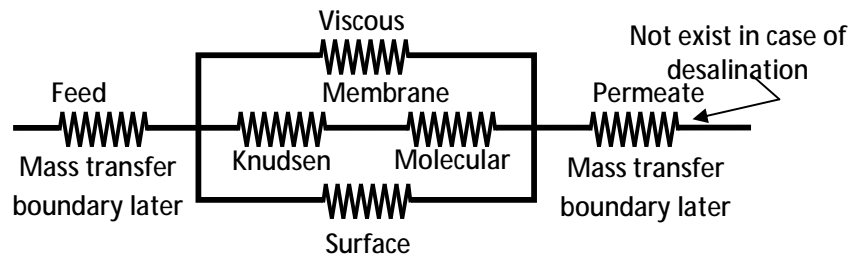
Theoretical modeling

Mass transport across the membrane occurs in three regions depending on the pore size and the mean free path of the transferring species[40]: Knudsen region, continuum region (or ordinary-diffusion region) and transition region (or combined Knudsen/ordinary- diffusion region). [40-41]

As shown in Figure 2, the composition of non-volatile component increases from x^F to x_M^F in the concentration boundary layer. Various types of mechanisms have been proposed for controlling the transport of vapor through porous membranes. These mechanisms are may be one or more (combination) of three basic mechanisms, which are Knudsen diffusion, Poiseuille flow (viscous flow) and molecular diffusion. This

gives rise to several types of resistances to mass transfer resulting from these mechanisms of mass transfer (Figure 4a)[2]. In fact, these mechanisms are depending on the pore size and the mean free path of the transferring species across the membrane in DCMD process. Across the membrane there are three mechanisms of mass transport may be occur: Knudsen region, continuum region (or ordinary-diffusion region) and transition region (or combined Knudsen/ordinary- diffusion region). In DCMD process, the viscous flow is negligible since both the feed and the permeate are contact with the membrane under atmospheric pressure, so that the total pressure is constant at about 1 atm[2,40-41]. The surface diffusion is insignificant for pore size $> 0.02 \mu\text{m}$ [14] this pore size is less than the usual pore size used in MD process. Knudsen number ($\text{Kn} = \lambda/d$) is a guideline in determining which mechanism is operative under a given experimental conditions. If $\text{Kn} > 1$ (i.e., $d < \lambda$), Knudsen type of flow will be the prevailing mechanism that describes the water vapor transport through the membrane pores (i.e., the molecule-pore wall collisions are dominant over the molecule-molecule collisions). If $\text{Kn} < 0.01$ (i.e., $d > 100 \lambda$), molecular diffusion is used to describe the mass transport in continuum region caused by the virtually stagnant air trapped within each membrane pore due to the low solubility of air in water. Finally, in the transition region, $0.01 < \text{Kn} < 1$, the mass transport takes place via the combined Knudsen/ordinary- diffusion mechanism (i.e., water collide with each other and diffuse among the air molecules). Usually in DCMD the combination of Knudsen diffusion and molecular diffusion of vapor transport through the membrane pores is almost responsible for mass transport, according to the usual pore diameters for most membrane used in DCMD, and to the molecular mean free path of water vapor in air. [1,40-42]

With respect to the basic principles of heat transfer, if the temperatures of fluid and solid surface are different, a thermal boundary layer will be formed when a fluid is brought into contact with a solid surface. The thermal boundary layer is adjacent to the solid surface, and it is assumed that only in this region, the fluid exhibits its temperature profile. This viewpoint is adopted to describe the MD process. Within the MD module, two fluids with different temperatures are separated by a microporous membrane (with the thickness of δ), therefore two thermal boundary layers appear at the feed side and the permeate side of the membrane, respectively as shown in Figure 2. The heat inside the membrane is transferred by two ways: one by conduction across the membrane material (heat losses), and the other way together with a vapor flowing through the membrane (see Figure 4b).



Figure(4a): Electrical analogy circuit presenting the mass transfer resistances in MD

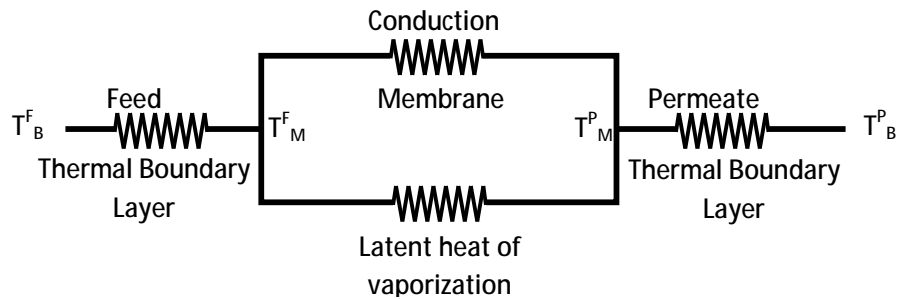


Figure (4b): Electrical analogy circuit presenting the heat transfer resistances in MD

The analysis of the modeling procedure was based on dividing each single fiber in the module into N elements, each element acts as mini DCMD as presented in the previous work [42].

The assumptions that are considered in the present model were, the rejection of the nonvolatile component in the feed is 100% due to there is no wetting occurs through pores. Mechanical equilibrium (constant total pressure) for the vapor and liquid phases with thermodynamic equilibrium between them (corresponding to the temperature) occurs at the interface at both feed and permeate side. The mechanisms of viscous (Poiseuille) flow across the membrane is neglected because of the total pressure is constant along the water transport path of about 1 atm. The water vapor diffuses through the static entrapped air in the pores. Due to low solubility of air in water the air is assumed insoluble in water. The pore size for whole membrane is uniform (neglected pore size distribution).

The summary of the main equations used for the modeling are listed below;

Heat transfer

$$Q_i^F = h_i^F A_{ro} (\bar{T}_{Bi}^F - T_{Mi}^F) + J_i A_{ro} H_i^{FV} \tag{2}$$

$$Q_i^F = m_{i-1}^F H_{i-1}^L - m_i^F H_i^L - J_i A_{ro} H_i^{FV} \tag{3}$$

$$Q_i^P = h_i^P A_{ri} (T_{Mi}^P - \bar{T}_{Bi}^P) + J_i A_{ro} H_i^{PV} \tag{4}$$

$$Q_i^P = m_{i-1}^P H_{i-1}^L - m_i^P H_i^L + J_i A_{ro} H_i^{PV} \tag{5}$$

$$Q_i^M = h_i^M A_{rln} (T_{Mi}^F - T_{Mi}^P) + J_i A_{ro} (H_i^{FV} - H_i^{PV}) \tag{6}$$

$$Q^F = Q^M = Q^P \tag{7}$$

$$J_i = -k_i^F C_T M w t_w \ln \left(\frac{x_{Mi}^F}{\bar{x}_{Bi}^F} \right) \tag{8}$$

$$x_{Bi}^F = \frac{m_{i-1}^F (Mwt_{sol})_i}{m_i^F (Mwt_{sol})_{i-1}} x_{Bi-1}^F \quad (9)$$

$$m_{i-1}^F = m_i^F + J_i A_{ro} \quad (10)$$

$$m_{i-1}^P = m_i^P - J_i A_{ro} \quad (11)$$

$$J_i = K_i^M (p_{Mi}^F - p_{Mi}^P) \quad (12)$$

Equation (2) gives the net of heat transferred in the boundary layer of the outer membrane surface which is by convection and water vapor leaving the boundary layer. Based on the sensible enthalpy difference between the inlet and outlet of the main feed stream and the enthalpy of the water vapor transported to membrane side energy balance in the feed side can be written as Eq. (3). Equation (4) describe the heat is transferred by convection and mass transfer contribution in thermal boundary layer in the permeate side (inner surface). The energy balance in the permeate side is given by Eq. (5) which describe the sensible heat difference between the inlet and outlet of the main permeate stream and the enthalpy of the water vapor transported from membrane side. The heat transfer across the membrane is by conduction (in solid and fluid) and water vapor transports across the membrane through the pores as Eq. (6). And at steady state Eq. (7) describes the whole heat transfers.

According to the theory of mass transfer in boundary layer the mass flux of species (volatile component) through the concentration boundary layer of nonvolatile component may be calculated from Eq. (5). A component mass balance on the nonvolatile component in the feed side yields Eq. (9). The total mass balance in the feed and permeate sides are given by Eqs. (10) and (11) respectively. Finally the mass transfer in the DCMD process is usually described by assuming a linear relationship between the mass flux (J) and the water vapor pressure difference through the MDC (KMi) as given by Eq. (12).

The set of simultaneous nonlinear equations resulted from heat and mass balances on each cell of a train of a multicells, is solved numerically using a developed program written by MATLAB® code. The parameters that are used as input data were the inlet temperature and mass flow rate of the feed and permeate side stream, and the inlet salt concentration of the feed side stream. The printout of the developed program for each cell are; at the feed side: outlet temperature, mass flow rate, the membrane surface temperature and salt concentration, whereas, at the permeate side: outlet temperature, mass flow rate, and the membrane surface temperature as well as the permeation flux and the rate of heat transferred across the membrane.

To predict the ten-stated unknown's variables a system of 10 nonlinear equations has been solved simultaneously using the FSOLVE coding, which is a built-in function in MATLAB®. This coding uses the least square method as a numerical technique for solving a system of nonlinear equations.

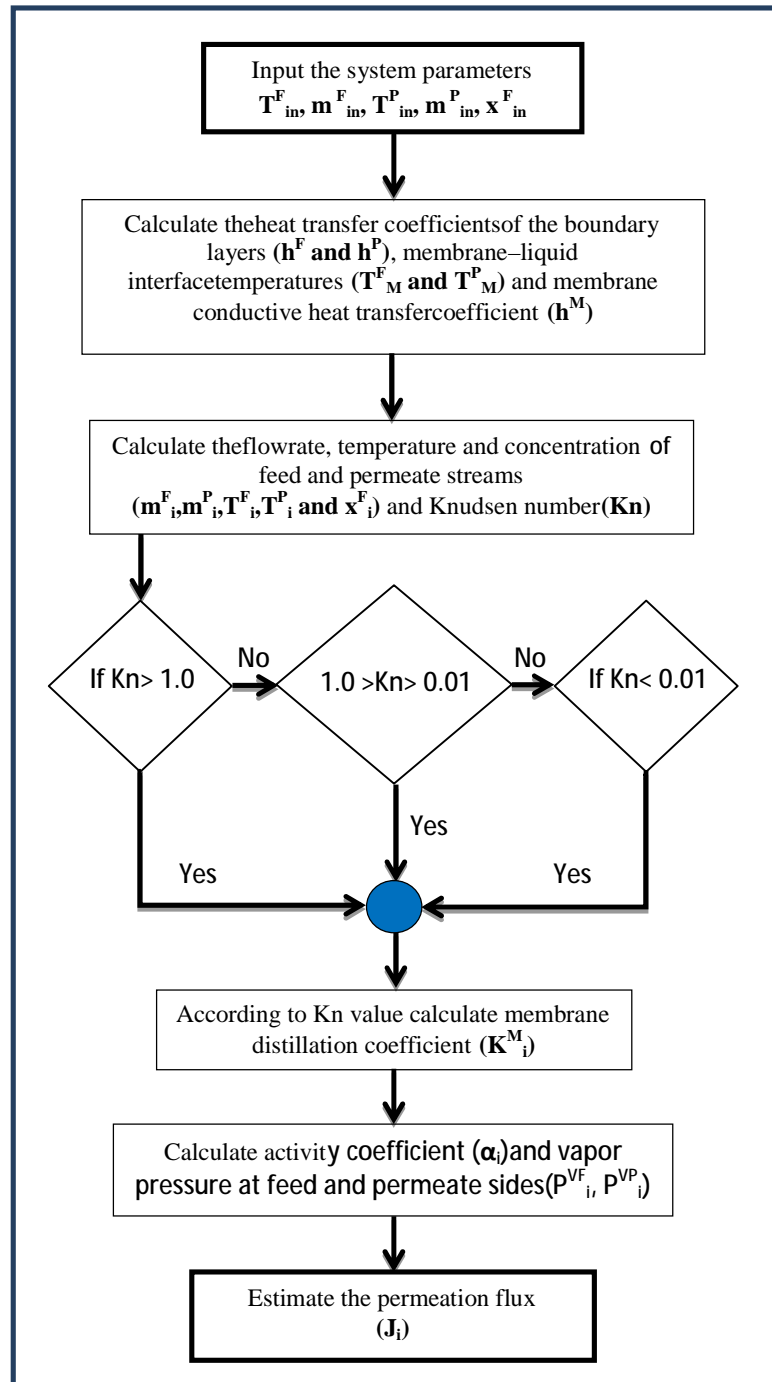


Figure (3): Flow chart of the algorithm used for DCMD modeling.

Results and Discussion

The effects of the membrane characterizations appeared in equation (1) are required to be studied in more attention to determine the precise effects of these parameters on the permeate flux in order to design membrane with optimum values of these characterizations that give higher permeation. The effects of these characterizations have been studied theoretically in the present study by simulation using a mathematical model. Verification the validity of this model was carried out through using a wide range of available experimental data of the permeation fluxes as a function of different feed temperatures, salt concentrations, flow rates of feed or permeate, membrane type, porosity, or pore diameter and also using the experimental values of outlet temperature of the feed and permeate streams. Very good to excellent agreement among the model predictions and these data[42]

An extensive study to predict the effect of changing individual parameters (design parameters) on permeate flux, such as the outside and inside diameters, the thickness of the hollow fiber membrane, the pore size, porosity, tortuosity, and the operating conditions, such as temperature, concentration and velocity of feed and permeate stream. The typical system used in this study as input feeding to the model was based on [1] as given in Table 1.

Table (1) the typical input data that feeding the model of DCMD that have experimental value of permeate flux of 31 kg/m² h.

Inlet feed temperature (°C)	70	Pore size (µm)	0.16
Inlet permeate temperature (°C)	20	porosity	0.8
Inside diameter (mm)	0.6	Shell diameter (mm)	9.5
Outside diameter (mm)	0.82	No. of fibers	65
Feed velocity (m/s)	1.6	Length (cm)	20
Permeate velocity (m/s)	0.8	Inlet feed concentration	3.5wt%

The effective parameters that affect the performance of DCMD could be divided into membrane characteristics, operating conditions, and parameters of module specifications. The effects of these parameters on the permeate flux across the membrane in hollow fiber modules are given below.

Effect of Outside Diameter of the Hollow Fiber Membrane

The effect of outside diameter of hollow fiber on the permeate flux is shown in Figure 5. It can be seen that at constant inside diameter, the permeate flux increases with increasing outside diameter until reaching maximum permeate fluxes at outside diameter between 605 to 630 µm or at optimum wall thickness

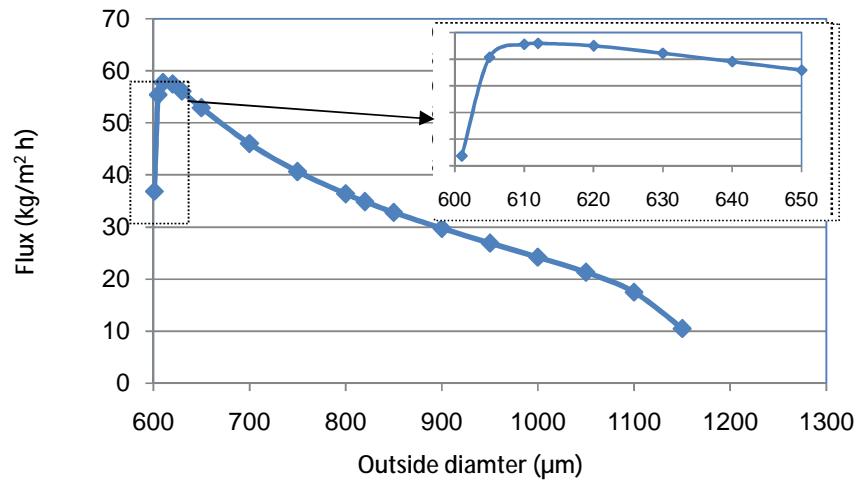


Figure (5): Effect of Outside Diameter of Hollow Fiber with Constant Inside Diameter on Permeate Flux.

That lies between 5 to 25 µm for the studied system (see Table 1) of 600 µm as an inside diameter. Then, the flux decays with increasing the outside diameter (increasing the wall thickness). This is maybe due to the degree of the resistances effect of each of mass and heat transfer across the membrane on the permeate flux.

The predictions trend of the present model with respect of the relation between the permeate flux and membrane thickness that shown in Figure (5) are agreed with that given in literature Figure (5a)[20] in terms of reaching maximum permeate fluxes at optimum wall thickness.

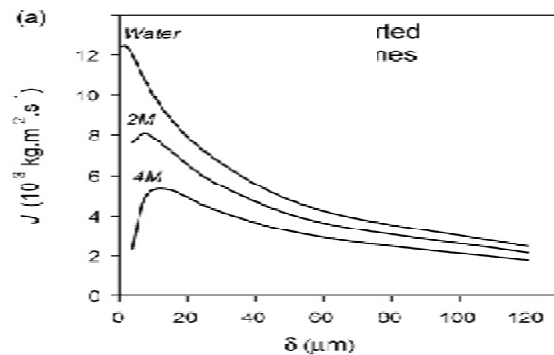


Figure (5a): Water Flux Vs. Membrane Thickness in the Treatment of Water, 2M and 4M NaCl Aqueous Solutions.[20]

Effect of Inside Diameter of the Hollow Fiber Membrane

Figure (6) shows the effect of the inside diameter of the hollow fiber membrane on the permeate flux. It can be noticed that, at constant outside diameter, the permeate flux increases with increasing inside diameter until reaching maximum fluxes at

inside diameter between 780 to 815 μm or at optimum wall thickness that lies between 5 to 40 μm for the studied system of 820 μm as an outside diameter. Then, the flux decays with increasing the inside diameter (decreasing the wall thickness). The reason is also due to the degree of the resistances effect of each of the mass and heat transfer resistance across the membrane on the permeate flux.

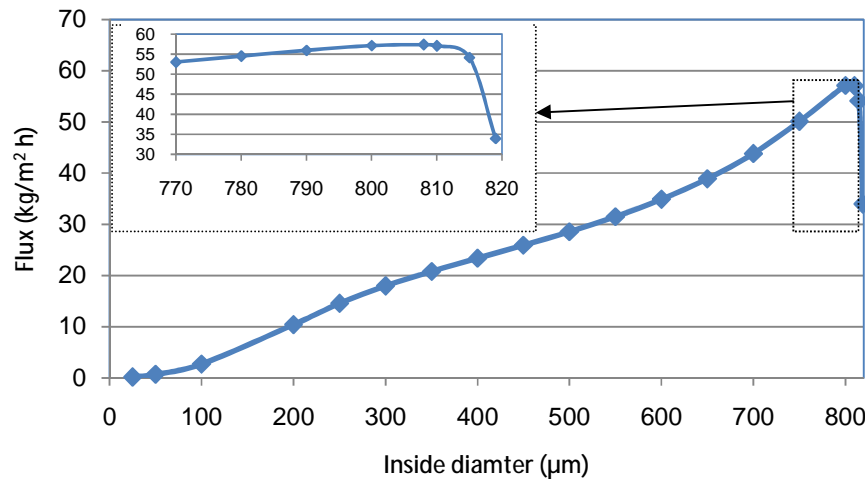


Figure (6): Effect of inside diameter fiber with constant outside diameter of hollow fiber on permeate flux

Effect of the Wall Thickness of the Hollow Fiber Membrane

Similar to other membrane processes, RO, UF, MF,...etc., membrane thickness has a significant effect on the overall mass transfer resistance in the MD process [11]. However, in contrast to other membrane approaches, the membrane permeation flux does not have a monotonically increasing trend as a function of membrane thickness reduction. This is because of the both effects of mass and heat transport phenomena on the permeate flux in DCMD. In fact, a smaller membrane thickness decreases the mass transfer resistance introduced by the membrane and leads to a higher permeate flux. While, as the membrane thickness decreases, a lower temperature gradient across the membrane, (i.e., lower driving force across the membrane) which leads to ultimately a lower permeate flux. Therefore, there should be an optimum thickness for the membranes depending on their other properties as well as the flow geometry [19]. In another words there is a competition between the resistances of mass and heat transfer that affect the permeate flux with changing of the membrane thickness. Figure 7 shows the effect of the membrane thickness on the permeate flux. It is clear that there is an optimum thickness for each inside or outside diameter of hollow fiber and versa vice (i.e., for each membrane thickness, there is an optimum inside or outside diameter of hollow fiber membrane). Figure 7 depicts that the membrane thickness of hollow fiber is one of several factors that affects the value of the permeate flux across the membrane but the selection of appropriate inside or outside diameter also plays an important role with membrane thickness for improving the permeate fluxes. For example, according to Figure 7, the permeate flux of hollow fiber membrane of 50 μm thickness and 600 μm inside diameter is higher than that of 5 μm thickness of 100 or 1100 μm inside diameter. Therefore, there is an optimum

membrane thickness for maximizing the water permeate flux across the membrane. This conclusion is agreed with Martinez, et al., [20] results. Moreover, it can be concluded that the optimum membrane thickness depends upon the inside or the outside diameter.

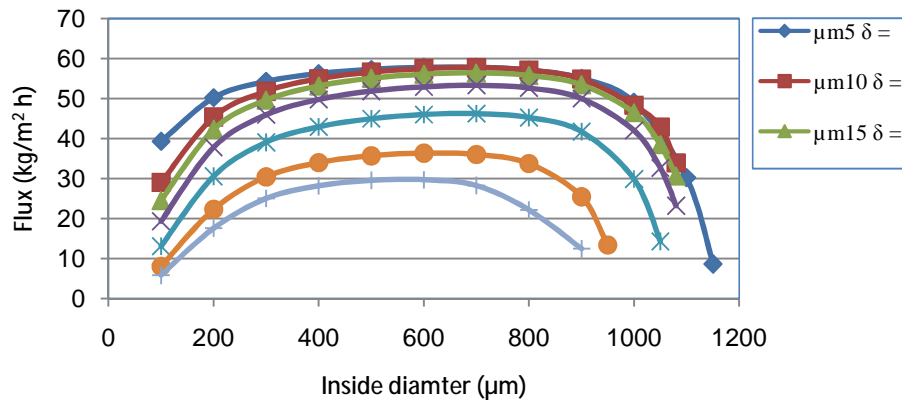


Figure (7): Effect of membrane thickness of hollow fiber on permeate flux

Effect of Pore Size

Reducing pore size may decrease the membrane surface porosity and increase tortuosity, which will produce a lower permeate flux. Therefore, the optimum membrane structures are with the decreased pore size and improved porosity to values ensure that the solution temperature, process pressure, and salt concentration fluctuations do not result in membrane wetting.

Figure 8 shows that the increasing of the pore size will improve the permeate flux across the membrane but the rate at which the flux increases decreases as the pore size increases till that the permeate flux has no significant effect and becomes independent on the pore size for membranes of high pore size. For the studied system, the pore sizes in the range of 0.3 to 0.6 µm are satisfied to give suitable high values of the permeate flux with respect to allowable pore size for membrane used in MD process.

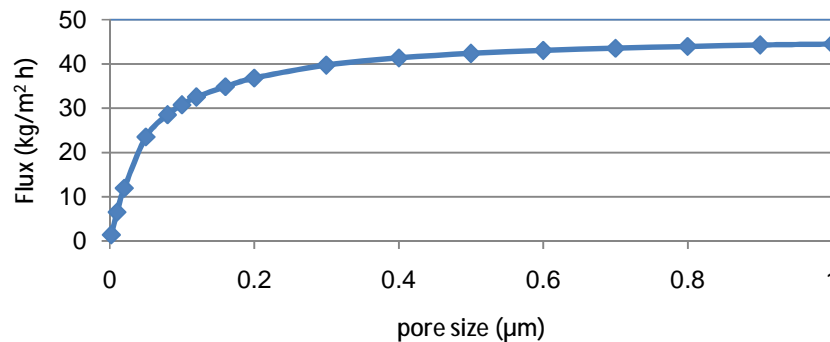


Figure (8): Effect of Pore Size of Hollow Fiber Membrane on Permeate Flux

Effect of Membrane Porosity

In general, for most studies, the MD membrane porosity lies between 30 and 85 %, and higher values of porosity lead to higher permeate fluxes [11]. Figure 9 shows that the permeate flux increases with increasing porosity, so high porosity always gives higher permeate flux, and the porosity has clearly more significant effect on the permeation flux than the pore size within their practical ranges. Higher membrane porosity corresponds to a larger diffusion area inside the membrane, which lessens the vapor transport resistance. In addition, higher porosity also reduces the amount of heat lost by conduction. [22].

Effect Of Membrane Tortuosity Factor

The membrane pores do not go straight across the membrane, and the diffusing molecules must move along tortuous paths, which lead to permeate fluxes decay. Figure 10 shows that the effect of the tortuosity factor on the MD fluxes, where it's clear that the flux decreases with increasing the tortuosity due to increase in mass transfer resistance. The value of tortuosity plays a very important role in the calculation of the permeate flux, in spite of that this value is mostly assumed depending on the prediction values of the permeate flux by a given mathematical model comparing with the experimental data. Whereupon, it is required a rigid and unified procedure for evaluation the tortuosity based on extensive experimental work. Figure 10 shows the prediction value of the permeate flux with varies assumed values of the tortuosity.

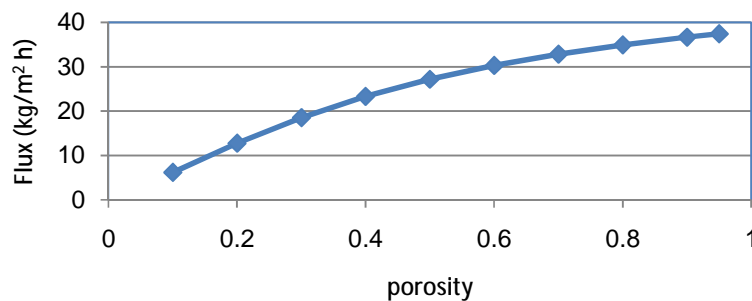


Figure (9): Effect of Porosity of Hollow Fiber Membrane on Permeate Flux

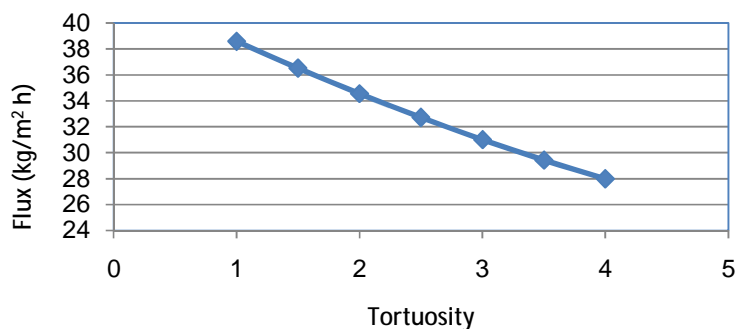


Figure 10: Effect of Tortuosity of Hollow Fiber Membrane on Permeate Flux

Effect of Temperature of the Feed and the Permeate

The effect of inlet temperatures of the feed stream on the permeate flux at constant inlet temperature of the permeate stream are shown in Figure 11. It is clear that in order to maximize the permeation flux, it is required to maximize the driving force for water vapor transport across the membrane through increasing the temperature difference (increase the vapor pressure difference) at the vapor/liquid interface in each side of the membrane. Figure 11 shows clearly, the exponential trend of permeate flux with the inlet feed temperatures at different inlet permeate temperature due to the exponential nature of the relationship between the temperature of the feed and permeate streams with the permeate flux based on the functional relation of the vapor pressure with temperature. Thus, it is more convenient to increase the inlet feed stream temperature rather than to decrease the permeate stream temperature in order to obtain higher permeate flux because of low variation of vapor pressure at low temperatures. In another words, at constant temperature difference between the feed and the permeate streams, the permeate flux increases when the temperature of the hot feed rises, which means the permeate flux is more dependent on the inlet feed temperature than the permeate temperature. This is due to that the constant temperature difference numerically does not mean constant vapor pressure difference. This fact is clear as shown in Figure 11a which illustrates that there is increasing in flux values with increasing feed temperature at constant temperature difference between the feed and permeate. Figure 11b shows the effect of the inlet permeate temperature on the permeate flux at constant inlet feed temperature. It is clear that there is a significant effect of the inlet permeate temperature on the permeate flux. In DCMD, the inlet temperature of the permeate stream is inversely proportional with permeation flux. This is due to decrease of the transmembrane vapor pressure as far as the feed temperature is kept invariable. These results are in agreement with many studies that showed the inversely effect of the inlet permeate temperature on the permeate flux. [9,14-15, 43- 45].

Effect of Inlet Concentration of the Feed and the Permeate

As mentioned previously, the highly concentrated solutions can be treated using MD process without suffering the large decay in permeability observed in other membrane processes, such as the pressure-driven membrane processes.

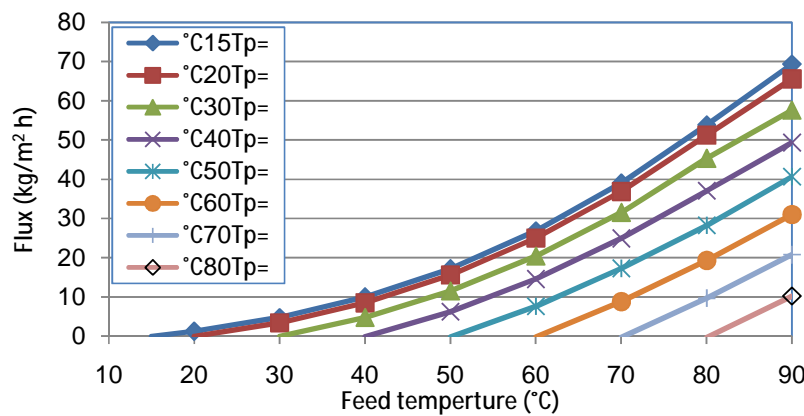


Figure (11): Effect of Inlet Feed Temperature on Permeate Flux at Constant Inlet Permeate Temperature.

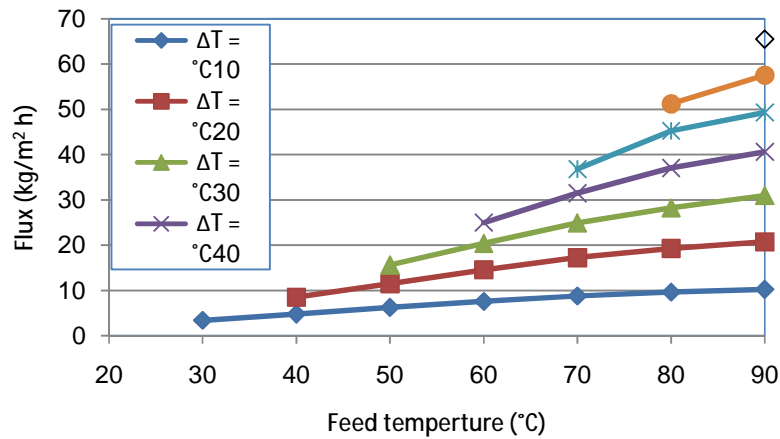


Figure (11a): Effect the Temperature Difference Between Feed and Permeate Stream on Permeate Flux

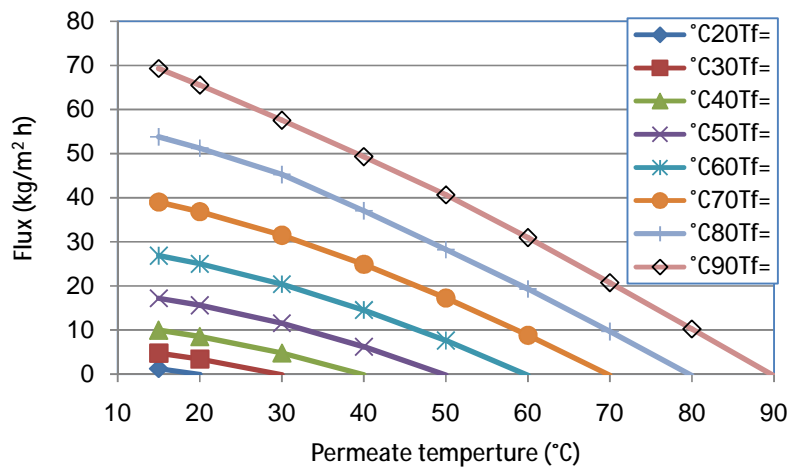


Figure (11b): Effect of Inlet Permeate Temperature on Permeate Flux at Constant Inlet Feed Temperature

The effect of inlet feed concentration on permeate flux is shown in Figure 12. It is clear from this figure that the significant effect of inlet feed concentration is when it is above 10 wt% (about 2M). This is attributed to the fact that the addition of salt to water reduces the partial vapor pressure and consequently reduces the driving force of water transport. This is obvious, since water vapor pressure is somewhat affected by salt concentration. For example, when the salt concentration in water is 10%, $\frac{p_{Solution}^V}{p_{Water}^V} = 0.94$; when the salt concentration reaches 20%, $\frac{p_{Solution}^V}{p_{Water}^V} = 0.85$, where p^V is the vapor pressure. There is also a contribution due to the effect of the concentration polarization (i.e., formation of a boundary layer on the feed membrane surface).

Nevertheless, this contribution is very small compared to that of the temperature polarization. [30,46].

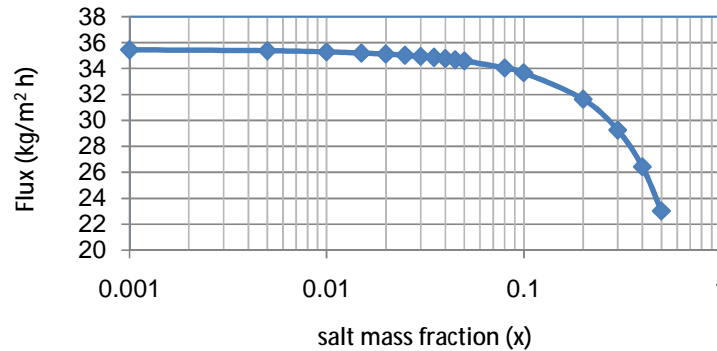


Figure (12): Effect of Inlet Feed Concentration on Permeate Flux.

Effect of Flowrate of the Feed and the Permeate

With increasing the flow rate of feed or permeate, the velocity of the fluid in these streams increases which leads to an improvement of mass and heat transfer in the bulk of the feed or the permeate side and in turn improve the permeate flux. This is due to increasing the heat and mass transfer coefficients in the boundary layer near the membrane surface in feed and permeate sides because of the increasing in Reynolds number. The membrane surface concentrations and temperatures will be brought closer to that of the bulk streams, and the trans-membrane temperature difference is thus increased. This led to reduce the temperature and concentration polarization effects. Figure 13 shows the effect of feed and permeate velocity on permeate flux. It is clear that the permeate flux increases with increasing the feed or permeate flow rate. However, the rate at which the flux increases decreases as feed or permeate flow rate increases. Figure 13 depicts that there are significant effects of permeate velocity at low velocities and no significant effects at high velocities of the permeate stream, while the effect of feed velocity continues at high velocities but with somewhat lower increasing rate of permeate flux. This is may be due to that in desalination process, there is no mass boundary layer at permeate side, and the heat transfer coefficient reaches the ultimate value that could be effective on the permeation flux at certain velocity of the permeate stream. Above this velocity, there are no more effects of permeate flowrate and the heat transfer coefficient on the permeate flux. While at feed side, there are thermal and mass boundary layers, which have continuous effective resistances with increasing the feed velocity, and their effects are somewhat lower at higher velocities. This discussion may explain the contrariety in the literature on the permeate velocity effect. Banat [31] found that the flow rates of permeate had no effect on the permeation flux, whereas many literature found that the permeate flux increases with the permeate flow rate [13,15,43,47]. The contrariety may be due to the studied region of the permeate velocity, as shown in Figure 13.

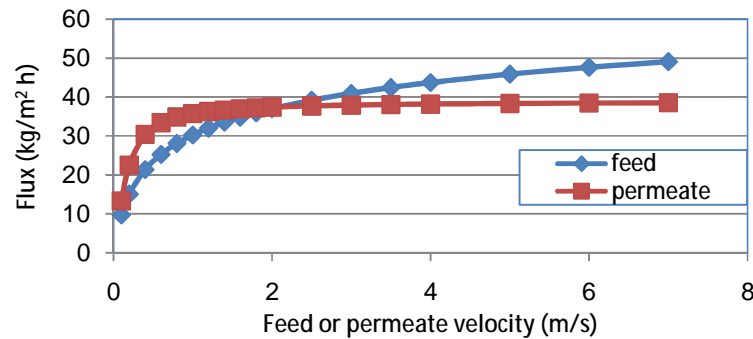


Figure (13): Effect of feed and permeate velocity on permeate flux

Effect of Length of the Module

Figure 14 shows the effect of the module length on permeate flux. It is clear from this figure that there is an inverse proportionality between the permeation flux and the module length. This result of the module length effect on the permeate flux agrees with experimental work of [8]. The decay of the permeate flux with the module length may be due to that the longer module length at a given inlet temperature and stream velocities lead to lower mean temperature difference across the membrane because of the increased residence time for heat and mass transfers. For MD process it is more suitable to use short module length since the risk of membrane pore wetting increased with the increased of fiber length because of the hydrostatic pressure drop along the length of the membrane module. [11].

Effect of Number of Fibers in the Module

In the reviewed literature, there is no study of the effect of this parameter, in spite of that this parameter has a significant effect on the permeate flux. Figure 15 shows the effect of the number of hollow fibers in the module. This figure reveals that the permeate flux increases with increasing the number of fibers in the module until reaching the maximum permeate flux at the optimum number of fibers which for the studied system was 57 fibers, and then the permeate flux decays with increasing the fibers. This may be due to that when the number of the fibers reaching 57 fibers which gives the maximum surface area for mass transfer above that number of the fibers the surface area decreases since any extra fibers inserted in the module will reduce the surface area at contact areas among other fibers.

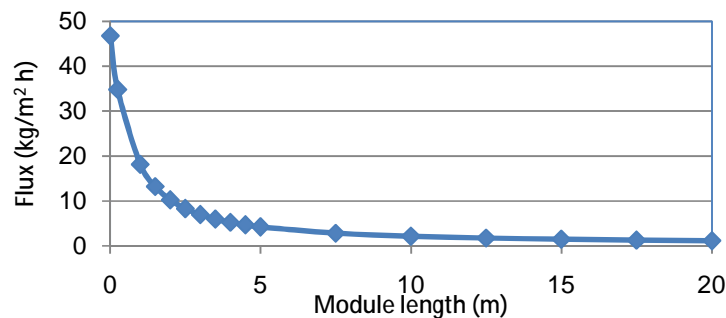


Figure 14: Effect of Module Length on Permeate Flux

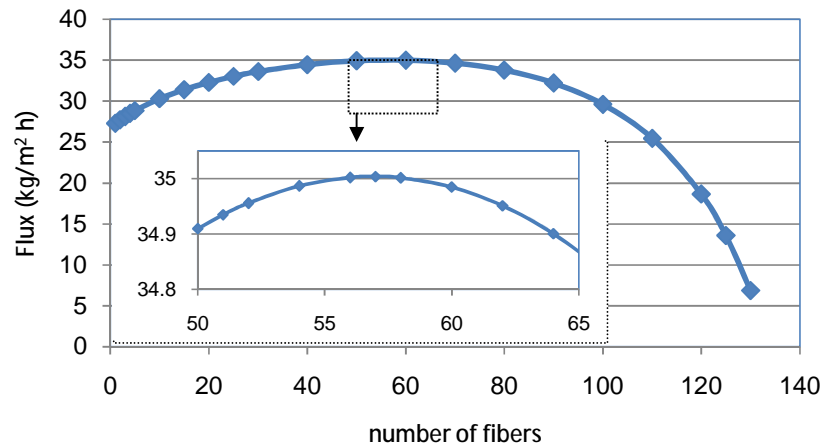


Figure (15): Effect of Number of Fibers in Module on Permeate Flux

CONCLUSIONS

This study concerns with an extensive investigation of the effective parameters on membrane distillation that may play important role to enhance the performance of the DCMD process. The influence of the outside and inside diameters, the thickness of the hollow fiber membrane, the pore size, porosity, tortuosity, module length, number of fibers in module, inlet feed temperature, inlet feed concentration, inlet permeate temperature and the velocity of feed and permeate streams have been investigated to maximize the permeate flux, and the following conclusions can be drawn:

- There is an optimum thickness for each inside or outside diameter of hollow fibers.
- Increasing the porosity and pore size within practical range and decreasing of tortuosity.
- Increasing the inlet feed temperature rather than decreasing the inlet permeate temperature for constant temperature difference between feed and permeate.
- The feed concentration and fiber length play an inverse role.
- The effect of increasing the feed and / or permeate flow rate is higher at low flow rate. And, there is no effect of permeate flow rate at higher rate.
- There is an optimum number of fibers in the module.

REFERENCES

- [1]. Kai Yu Wang, Tai-Shung Chung, and Marek Gryta, Hydrophobic PVDF hollow fiber membranes with narrow pore size distribution and ultra-thin skin for the freshwater production through membrane distillation, *Chem. Eng. Sci.* 63 (2008) 2587 – 2594.
- [2]. Abdullah Alkudhiri, Naif Darwish, and Nidal Hilal, Membrane distillation: A comprehensive review, *Desalination*, (2012), 287, 2-18.
- [3]. Shuguang Deng, Solar desalination of brackish water using membrane distillation process, New Mexico water resources research institute WRRRI Technical Completion Report No. 342, 2008.

- [4].J. Blanco Gálvez, L. García-Rodríguez, and I. Martín-Mateos, Seawater desalination by an innovative solar-powered membrane distillation system: the MEDESOL project, *Desalination* 246 (1–3) (2009) 567–576.
- [5].A.M. Alklaibi, and N. Lior, Transport analysis of air-gap membrane distillation, *J. Membr. Sci.* 255 (1–2) (2005) 239–253.
- [6].Liming Song, Baoan Li, Kamalesh K. Sirkar, and Jack L. Gilron, Direct Contact Membrane Distillation-Based Desalination: Novel Membranes, Devices, Larger-Scale Studies, and a Model, *Ind. Eng. Chem. Res.* 2007, 46, 2307-2323.
- [7].J. Zhang, N. Dow, M. Duke, E. Ostarcevic, J.-D. Li, and S. Gray, Identification of material and physical features of membrane distillation membranes for high performance desalination, *Journal of Membrane Science.* 349 (2010) 295-303.
- [8].Jianhua Zhang, Theoretical and experimental investigation of membrane distillation, PhD thesis Victoria University, Australia, 2011.
- [9].F.A. Banat, and J. Simandl, Desalination by membrane distillation: a parametric study, *Sep. Sci. Technol.* 33 (2) (1998) 201–226.
- [10].M. S. Khayet, and T. Matsuura, *Membrane Distillation: Principles and Applications*, Elsevier, 2010.
- [11].M.S. El-Bourawi, Z. Ding, R. Ma, and M. Khayet, A framework for better understanding membrane distillation separation process, *J. Membr. Sci.* 285 (2006) 4-29.
- [12].M. Gryta, M. Tomaszewska, J. Grzechulska, and A.W. Morawski, Membrane distillation of NaCl solution containing natural organic matter, Short communication, *Journal of Membrane Science* 181 (2001) 279–287.
- [13].M. Khayet, J.I. Mengual, and T. Matsuura, Porous hydrophobic/hydrophilic composite membranes: application in desalination using direct contact membrane distillation, *J. Membr. Sci.* 252 (2005) 101–113.
- [14].Kevin W. Lawson, and Douglas R. Lloyd, Review Membrane distillation, *J. Membr. Sci.* 124 (1997) 1–25.
- [15].F. Laganà, G. Barbieri and E. Drioli, Direct contact membrane distillation: modeling and concentration experiments, *J. Membr. Sci.*, 166 (2000) 1–11.
- [16].M. Khayet, J.I. Mengual, and T. Matsuura, Porous hydrophobic/hydrophilic composite membranes: application in desalination using direct contact membrane distillation, *J. Membr. Sci.* 252 (2005a) 101–113.
- [17].M. Khayet, T. Matsuura, and J.I. Mengual, Porous hydrophobic/hydrophilic composite membranes: estimation of the hydrophobic-layer thickness, *J. Membr. Sci.* 266 (2005b) 68–79.
- [18].L. Martínez, Comparison of membrane distillation performance using different feeds, *Desalination* 168 (2004) 359–365.
- [19].SinaBonyadi, and Tai Shung Chung, Flux enhancement in membrane distillation by fabrication of dual layer hydrophilic–hydrophobic hollow fiber membranes, *Journal of Membrane Science* 306 (2007) 134–146.
- [20].L. Martínez, and J.M. Rodríguez-Maroto, Membrane thickness reduction effects on direct contact membrane distillation performance, *J. Membr. Sci.* 312 (2008) 143.
- [20].M. S. Kim, S. J. Lee, J. U. Kang, and K. J. Bae, Preparations of Polypropylene Membrane with High Porosity in Supercritical CO₂ and Its Application for PEMFC, *Journal of Industrial and Engineering Chemistry.* 11 (2005) 187-193.
- [21].Z. Wang, Z. Gu, S. Feng, and Y. Li, Applications of membrane distillation technology in energy transformation process-basis and prospect, *Chinese Science Bulletin.* 54(2009) 2766-2780.

- [23].M. M. Teoh, and T.-S. Chung, Membrane distillation with hydrophobic macrovoid-free PVDF-PTFE hollow fiber membranes, *Separation and Purification Technology*. 66(2009) 229-236.
- [24].SurapitSrisurichan, RatanaJiratananon, and A.G. Fane, Mass transfer mechanisms and transport resistances in direct contact membrane distillation process, *Journal of Membrane Science* 277 (2006) 186–194.
- [25].J.S. Mackie, E. Meares, *Proc. R. Soc. A*232 (1955) 498.
- [26].R.W. Schofield, P.A. Hogan, A.G. Fane, and C.J.D. Fell, Developments in membrane distillation, *Desalination* 62 (1987) 728.
- [27].Drioli, E., Wu, Y., and Calabro, V., Membrane distillation in the treatment of aqueous solutions, *J. Membr. Sci.* 1987, 33, 277.
- [28].Schneider, K., Holz, W., and Wollbeck, R. Membranes and modules for transmembrane distillation. *J. Membr. Sci.* 1988, 39, 25.
- [29].M. Gryta, Influence of polypropylene membrane surface porosity on the performance of membrane distillation process. *Journal of Membrane Science* 287, (2007), 67.
- [30].L. Martínez-Díez, and M.I. Vázquez-González, Temperature and concentration polarization in membrane distillation of aqueous salt solutions, *J. Membr. Sci.* 156 (2) (1999) 265–273.
- [31].F. A. Banat, Membrane distillation for desalination and removal of volatile organic compounds from water, PhD Thesis, McGill University, Canada, (1994).
- [32].F.A. Banat, and J. Simandl, Theoretical and experimental study in membrane distillation, *Desalination* 95 (1) (1994) 39–52.
- [33].M. Qtaishat, T. Matsuura, B. Kruczek, and M. Khayet, Heat and mass transfer analysis in direct contact membrane distillation, *Desalination* 219 (2008) 272–292.
- [34].Y. Yun, et al., Direct contact membrane distillation mechanism for high concentration NaCl solutions, *Desalination* 188 (1–3) (2006) 251–262.
- [35].M.A. Izquierdo-Gil, M.C. García-Payo, and C. Fernández-Pineda, Air gap membrane distillation of sucrose aqueous solutions, *J. Membr. Sci.* 155 (2) (1999) 291–307.
- [36].T.C. Chen, C.-D. Ho, and H.-M. Yeh, Theoretical modeling and experimental analysis of direct contact membrane distillation, *J. Membr. Sci.* 330 (1–2) (2009) 279–287.
- [37].Shojikubota Kubota, et al., Experiments on seawater desalination by membrane distillation, *Desalination* 69 (1) (1988) 19–26.
- [38].SinaBonyadi, and Tai-Shung Chung, Highly porous and macrovoid-free PVDF hollow fiber membranes for membrane distillation by a solvent-dope solution co-extrusion approach, *Journal of Membrane Science* 331 (2009) 66–74.
- [39].M.M. Teoh, S. Bonyadi, and T.S. Chung, Investigation of different hollow fiber module designs for flux enhancement in the membrane distillation process, *J. Membr.Sci.* 311 (2008) 371.
- [40].J. Phattaranawik, R. Jiratananon, and A.G. Fane, Effect of pore size distribution and air flux on mass transport in direct contact membrane distillation, *J. Membr. Sci.*, 215 (2003) 75–85.
- [41].M. Khayet, Velazquez, A., and Mengual, J.I., Modeling of mass transport through a porous partition: Effect of pore size distribution, *Non-Equilibrium Thermodynamics*, 29 (2004) 279-299.

- [42].Salah S. Ibrahim and Qusay F. Alsahy, Modeling and Simulation for Direct Contact Membrane Distillation in Hollow Fiber Modules, AIChE Journal February 2013 Vol. 59, No. 2, 589-603.
- [43].M. Khayet, M. P. Godino, and J. I. Mengual, Possibility of nuclear desalination through various membrane distillation configurations: a comparative study. International Journal of Nuclear Desalination 1 (1),(2003), 30-46.
- [44].Kevin W. Lawson, and Douglas R. Lloyd, Membrane Distillation. II. Direct contact MD, J. Membr. Sci. 120 (1996) 123–133
- [45].M. Matheswaran, et al., Factors affecting flux and water separation performance in air gap membrane distillation, J. Ind. Eng. Chem. 13 (6) (2007) 965–970.
- [46].M. Khayet, M.P. Godino, and J.I. Mengual, Study of asymmetric polarization in direct contact membrane distillation, Sep. Sci. Technol. 39 (1) (2004a) 125–147.
- [47].Ohta, K., Kikuchi, K., Hayano, I., Okabe, T., Goto, T., Kimura, S., et al. Experiments on sea water desalination by membrane distillation. Desalination, (1990), 78, 177-185.